Environmental Science & Technology

pubs.acs.org/est

Article

Fuel-Type Independent Parameterization of Volatile Organic Compound Emissions from Western US Wildfires

Kanako Sekimoto,* Matthew M. Coggon, Georgios I. Gkatzelis, Chelsea E. Stockwell, Jeff Peischl, Amber J. Soja, and Carsten Warneke

Cite This: *Environ. Sci. Technol.* 2023, 57, 13193−13204

Read Online

ACCESS | Metrics & More | Article Recommendations | Supporting Information

ABSTRACT: Volatile organic compounds (VOCs) emitted from biomass burning impact air quality and climate. Laboratory studies have shown that the variability in VOC speciation is largely driven by changes in combustion conditions and is only modestly impacted by fuel type. Here, we report that emissions of VOCs measured in ambient smoke emitted from western US wildfires can be parameterized by high- and low-temperature pyrolysis VOC profiles and are consistent with previous observations from laboratory simulated fires. This is demonstrated using positive matrix factorization (PMF) constrained by high- and low-temperature factors using VOC measurements obtained with a proton-transfer reaction time-of-flight mass spectrometer (PTR-ToF-MS) on board the NASA DC-8 during the FIREX-AQ (Fire Influence on Regional and Global Environments and Air Quality) project in 2019. A linear combination of high- and low-temperature factors described more than 70% of the variability of VOC emissions of long-lived VOCs in all sampled wildfire plumes. An additional factor attributable to atmospheric aging was required to parameterize short-lived and secondarily produced VOCs. The relative contribution of the PMF-derived high-temperature factor for a given fire plume was strongly correlated with the fire radiative power (FRP) at the estimated time of emission detected by satellite measurements. By combining the FRP with the fraction of the high-temperature PMF factor, the emission ratios (ERs) of VOCs to carbon monoxide (CO) in fresh wildfires were estimated and agree well with measured ERs (r^2 = 0.80−0.93).

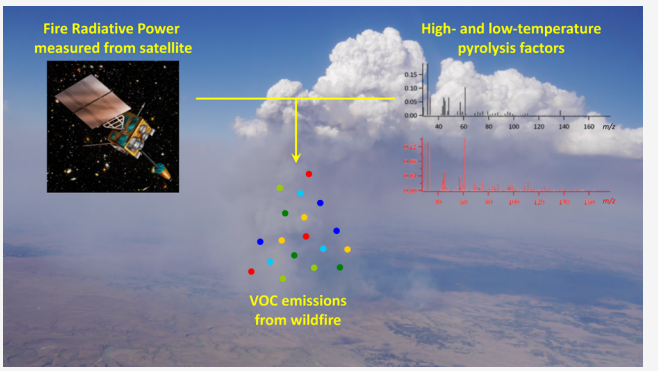

KEYWORDS: *wildfire, volatile organic compound (VOC), proton-transfer reaction time-of-flight mass spectrometry (PTR-ToF-MS), high-temperature pyrolysis, low-temperature pyrolysis, fire radiative power (FRP), FIREX-AQ, positive matrix factorization (PMF)*

INTRODUCTION

Wildfires are an important natural event in many ecosystems, but the resulting emissions cause poor air quality on regional to continental scales[1−3] and adversely impact human health.[4,5] The frequency and intensity of wildfire activity in the western United States are expected to increase in the future due to a combination of widespread population growth in the wildland−urban interface and climate change.[6,7] Therefore, it is important to understand both qualitatively and quantitatively the chemical composition and the magnitude of wildfire emissions to accurately predict the effects of smoke on air quality and climate.

Biomass burning is a significant emission source of volatile organic compounds (VOCs), which can act as precursors to secondary pollutants such as ozone and secondary organic aerosol (SOA).[8−11] Several VOCs, such as benzene and isocyanic acid, can also have direct effects on human and ecosystem health.[12,13]

Numerous studies have quantified emission ratios and emission factors for various fuel types across burn conditions using field measurements from wildland and prescribed fires[14−20] or laboratory measurements from simulated burns.[21−23] Literature reviews have been periodically conducted to consolidate these results and provide recommended emission factors that can be applied to atmospheric models.[24−26] Nevertheless, uncertainties in the process-level understanding and model representation of fire emissions, plume rise, and chemistry still exist, which makes it difficult to accurately predict the VOC composition of primary biomass burning emissions in models. This can be caused by an insufficient understanding of the chemistry and total emissions of VOCs across fuel types, ecosystems, and/or fire combustion conditions.[27−29] VOC emissions from biomass burning are described by multiple

Received: January 19, 2023
Revised: August 4, 2023
Accepted: August 4, 2023
Published: August 23, 2023

complex processes that often occur simultaneously, e.g., distillation, pyrolysis, flaming, and smoldering combustion processes.[30−33] The relative importance of each process can change over the course of a fire and modulate the relative distribution of VOC emissions spatially and temporally and also relates to the variability in integrated VOC emissions between different fires. This variability has been often parameterized by flaming and smoldering processes as described by the modified combustion efficiency ($MCE = \Delta CO_2/(\Delta CO + \Delta CO_2)$),[30] and good correlations between MCE and emissions of some VOCs or total VOC emissions have been reported in lab and field measurements.[16,18,20,22,23,26,28,31]

Recently, Sekimoto et al.[34] applied positive matrix factorization (PMF) to VOC measurements from a proton-transfer-reaction time-of-flight mass spectrometer (PTR-ToF-MS) deployed during the FireLab 2016 experiment (at the US Forest Service Fire Sciences Laboratory) and found that VOC emissions from laboratory simulations of western US wildfires can be well described by just two fundamental processes: high- and low-temperature pyrolysis. The VOC profiles (or "factors") derived by PMF represented the linear combination of these processes and described on average 85% of the variability of the VOCs measured by PTR-ToF-MS. The high-temperature factor was found to be relatively enriched in aliphatic unsaturated hydrocarbons, (polycyclic) aromatic hydrocarbons, hydrogen cyanide (HCN), isocyanic acid (HNCO), and nitrous acid (HONO), while the low-temperature factor was dominated by aromatic oxygenates, furans, and ammonia (NH_3).[34] These factors, and the processes that define them, were observed across a diverse range of fuel types from ecosystems representative of boreal forests, temperate forests, grasslands, and chaparral.

"High-temperature" and "low-temperature" pyrolysis processes do not correspond exactly to the commonly used "flaming" and "smoldering" categories as described by MCE and are not well correlated with MCE. The reason is that most VOCs are emitted from pyrolysis of fuel biopolymers such as cellulose, hemicellulose, and lignin and *not* from the flaming and/or other combustion processes that are the main source of CO_2. Therefore, the two pyrolysis profiles are more appropriate to estimate VOC emissions from wildfires than MCE using CO_2 emissions.

In this study, we build upon the work described by Sekimoto et al.[34] on laboratory fires and parameterize the VOC emissions from real-world wildfires using VOC measurements from the NOAA PTR-ToF-MS conducted on board the NASA DC-8 during the 2019 FIREX-AQ campaign (Fire Influence on Regional and Global Environments and Air Quality).[35] We conduct a constrained PMF analysis and show that the high- and low-temperature pyrolysis factors obtained in the FireLab 2016 experiment describe the variability of many VOCs emitted from western US wildfires, independent of fuel type. We show that the relative abundance of the high-temperature factor correlates well with fire radiative power (FRP) data from the Geostationary Operational Environmental Satellite (GOES) satellites. Together, these results provide a framework to estimate VOC/CO emission ratios using satellite data that can be used to parameterize wildfire emissions in atmospheric models.

MATERIAL AND METHODS

FIREX-AQ Campaign Descriptions. This study utilizes measurements collected during the western portion of the FIREX-AQ field campaign that spanned 12 flights sampling 8 wildfires from July 22 to August 16, 2019 using the NOAA PTR-ToF-MS on board the NASA DC-8 aircraft.[35] The measurements were mainly performed during afternoon to evening. In this paper, sampling time is described by UTC. Local time is UTC-6 (MDT) or UTC-7 (PDT). Most flights were designed to sample background mixing ratios, fresh emissions near the fire source, and aged smoke as the emissions transported and diluted downwind. The aircraft first flew upwind of the fire to characterize ambient conditions unaffected by fire emissions. Subsequent cross-wind plume transects were conducted as close as possible to the fire to sample the emissions with minimal atmospheric aging.[20] The aircraft then transected the smoke plume successively further downwind at approximately 15−40 km intervals. Plume transects were designed to be perpendicular to the wind direction and through the center of the vertical extent of the plume, terrain permitting. The vertical structure of the plume was systematically assessed using a differential absorption lidar during a lengthwise overpass above the plume. A typical flight pattern is shown in Figure S1.

VOC Measurements. The instrumental setup of the NOAA PTR-ToF-MS installed on board by the NASA DC-8 was the same as described by Koss et al.[21] during the FireLab measurements and was the same instrument used by Sekimoto et al.[34] to derive PMF factors for high- and low-temperature pyrolysis VOC profiles. Koss et al.[21] speciated VOC isomers measured by the PTR-ToF-MS using gas chromatography preseparation and reported isomer distributions for over 150 individual ion masses. Most of the VOC speciation observed in the FIREX-AQ campaign agrees with that in the FireLab measurements, but there are some differences between them. For example, Koss et al. reported, at $[C_5H_6O + H]^+$ (m/z 83.0491), 51% of the signal resulted from 2-methylfuran, 9% resulted from 3-methylfuran, and 37% resulted from unidentified isomers + fragments of higher masses; however, the isomer distributions observed in the FIREX-AQ campaign were 16% from 2-methylfuran, 3% from 3-methylfuran, and 81% from unidentified isomers + fragments. These differences are largely attributed to the chemical oxidation that occurs between emission and sampling, which alters the VOC profiles and isomer distributions measured by PTR-ToF-MS.[18,20] More details on the VOC measurements and speciation by the NOAA PTR-ToF-MS during the FIREX-AQ campaign, as well as the impacts of chemistry of VOC speciation measured by aircraft, can be found elsewhere.[20,36]

FRP Measurements. FRP was measured at the fire source using Advanced Baseline Imager (ABI) instruments aboard the Geostationary Operational Environmental Satellite (GOES) satellites at a 5 min temporal and 2 km spatial resolution and varied significantly on these 5 min timesteps (https://www.goes-r.gov/spacesegment/abi.html).[37,38] The FRP observations were included within 4 km of the final GeoMac fire perimeter and data products from all FIREX-AQ sampled fires are archived in the NASA data archive (https://www-air.larc.nasa.gov/cgi-bin/ArcView/firexaq). The FRP product was interpolated onto a one second time-base to match the PTR measurement resolution. To relate in situ aircraft emissions to GOES FRP at the fire source, the time of emission is calculated from the smoke age. Smoke age is determined as the time elapsed from smoke production until measurement by the aircraft and is estimated from average wind speed and distance from the fire source or using trajectory models that implement high-resolution meteorological datasets and an assumed vertical transport.[35,36] The time of emission is estimated as the time of sampling minus the calculated smoke age. The average FRP across each plume

https://doi.org/10.1021/acs.est.3c00537
Environ. Sci. Technol. 2023, 57, 13193−13204

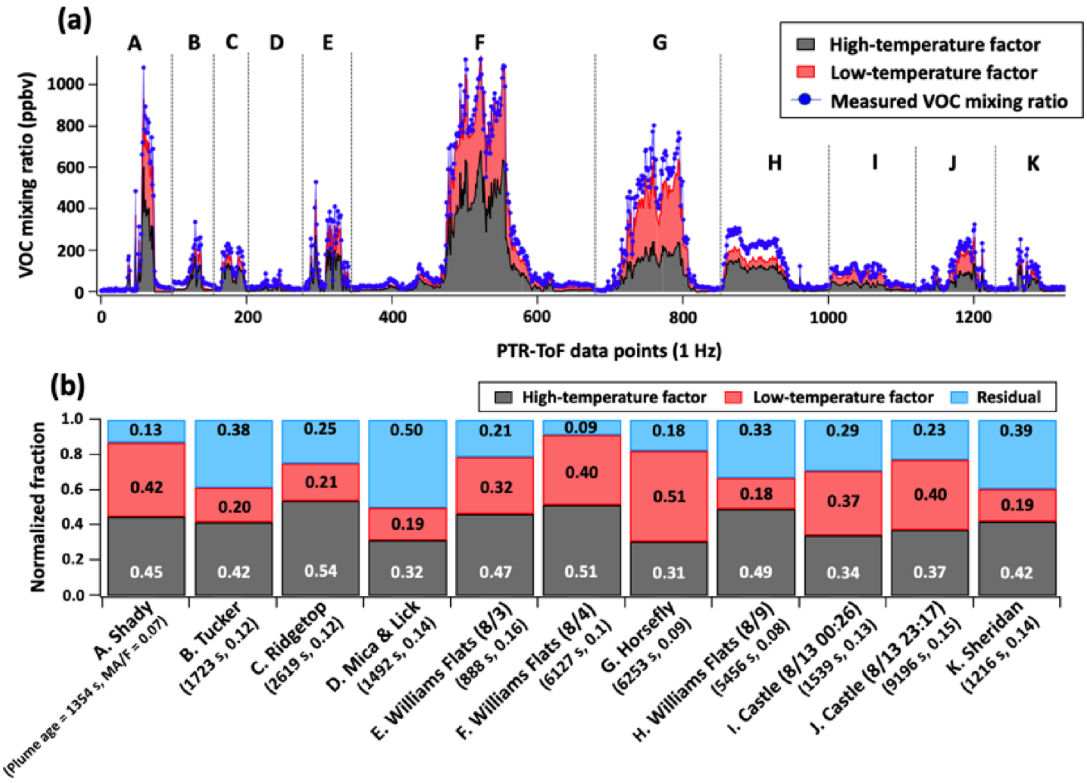

Figure 1. Two-factor PMF solutions of the freshest plumes for eight wildfires fully constrained by the high- and low-temperature pyrolysis factors. (a) Sum of all PTR-ToF-MS-measured VOC mixing ratio signals from 134 masses (blue line) and PMF fits (black and red area). (b) Normalized fractions of high-temperature factor, low-temperature factor, and residuals on a transect-integrated basis. The plumes were selected with young plume age (0.25−2.6 h) and low maleic anhydride/furan ratio (MA/F = 0.07−0.16).

transect emission window was estimated and then averaged together with additional transects to estimate a fire-averaged FRP for selected emission windows.

CO Measurements. CO was measured by cavity enhanced absorption using a modified Los Gatos Research/ABB CO/N_2O analyzer. Data were recorded at 5 Hz and reported at 1 Hz. More instrument details may be found in the work of Bourgeois et al.[39]

PMF Analysis. PMF is a numerical method that apportions the time series of various ion masses to different sources represented by factor profiles, factor time series, and residual signal unsolved by PMF. In this study, PMF was conducted using the Source Finder (SoFi) software,[40] which employs the Multilinear Engine (ME-2)[41] capable of performing fully or partially constrained PMF runs using known factor profiles (in this case the high- and low-temperature pyrolysis factors from Sekimoto et al.[34]).

Here, we applied PMF to PTR-ToF-MS data collected from 132 plume transects of 8 wildfires sampled by the DC-8 aircraft. This subset of transects encompassed a range of vegetation types including timber, grass, dead trees, logging brush, litter, etc., and physical plume ages from around 16 min to more than 5.5 h.

The original profiles of the high- and low-temperature factors consist of 574 ion masses,[34] but only 134 ion masses are used in this study (Table S1). These 134 masses were identified in laboratory smoke by Koss et al. using gas chromatography preseparation[21] and account for ∼80% of the total ion signal measured by PTR-ToF-MS. Using the FireLab measurement dataset, we confirm that PMF using only the 134 ion masses returns very similar results as obtained from the 574 ion masses used by Sekimoto et al.[34] (Figure S6). This indicates that those 134 ion masses are sufficient to describe PTR-ToF-MS measurements of VOC emissions and variability from biomass burning in the western US. Full details on preparation of PMF datasets are described in the SI.

RESULTS AND DISCUSSION

Smoke sampled in the field differs from smoke sampled in the laboratory because additional processes, such as atmospheric oxidation, can alter the chemical distribution of VOCs. Sekimoto et al. derived a 2-factor solution based on laboratory emissions that represent chemically fresh emissions,[34] while those presented here may have undergone chemical oxidation in the time between emission and sampling by the DC-8. To determine the optimal number of factors that best describe PTR-ToF-MS measurements of western US wildfire emissions, various PMF setups were run using several datasets with PTR-ToF-MS data that varied by plume transect selection and/or by selected VOC species (Scheme S1). As a result, we use three PMF configurations intended to isolate the effects of chemistry from variability associated with emissions for the 134 ions analyzed here.

These configurations include (1) 2-factor PMF run on the freshest smoke plumes that had limited photochemical aging. All compounds were included in this analysis, and the 2-factor solution was fully constrained with the high- and low-temperature factors following Sekimoto et al.,[34] (2) 2-factor PMF run on all plumes, fresh and aged, but only 22 long-lived compounds were included and the 2-factor solution was fully constrained with the high- and low-temperature factors, and (3) 3-factor PMF run on all plumes, fresh and aged, but only short-lived and secondary compounds were used. The high- and low-temperature factors were fully constrained, and the third factor

https://doi.org/10.1021/acs.est.3c00537
Environ. Sci. Technol. 2023, 57, 13193−13204

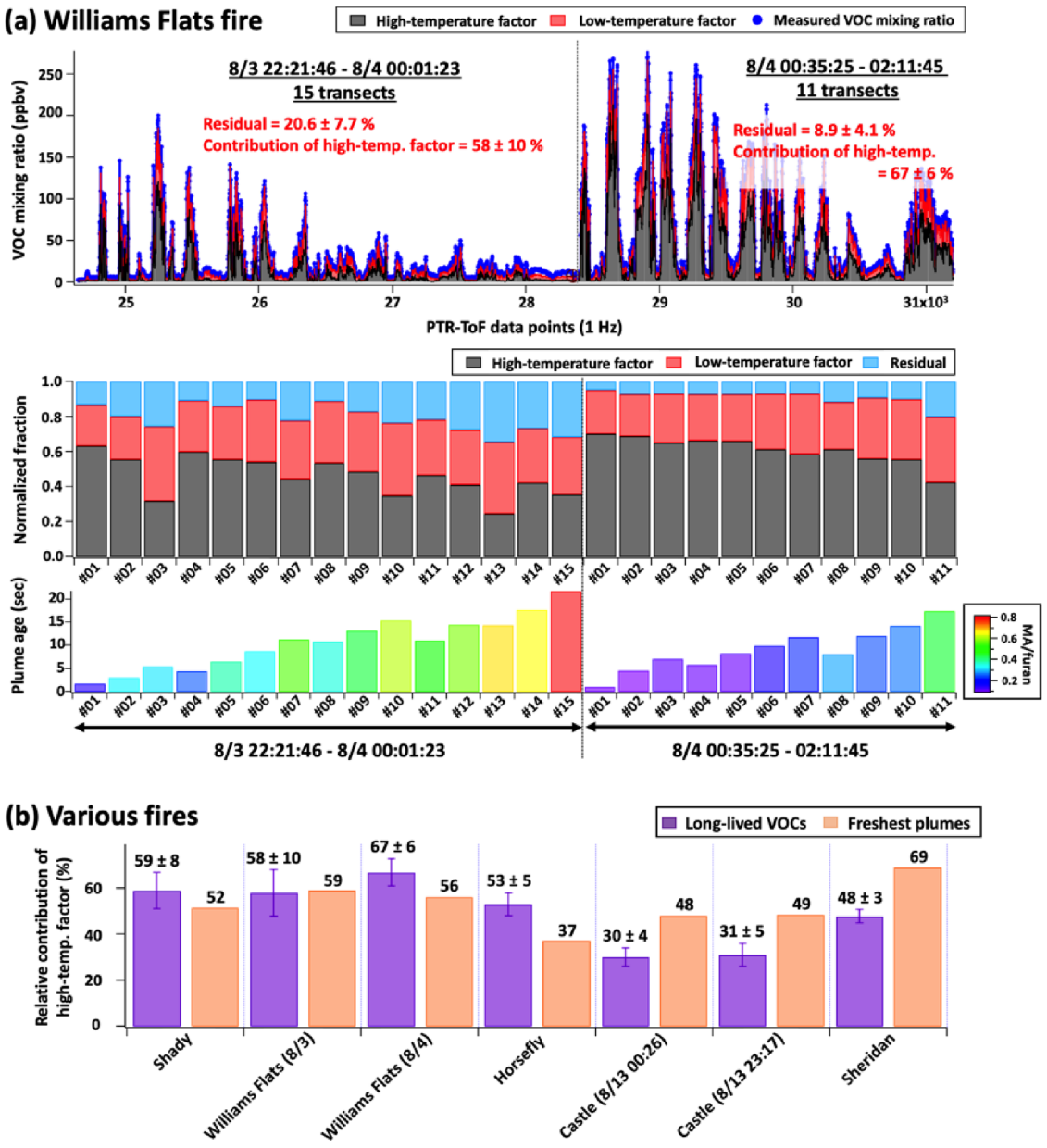

Figure 2. Two-factor PMF solution using 22 long-lived VOCs fully constrained by the high- and low-temperature pyrolysis factors. (a) Results for the Williams Flats fire (August 3rd and 4th, 2019): the sum of PTR-ToF-MS-measured total VOC mixing ratios and PMF fits (top panel), normalized fractions of the high-temperature factor, low-temperature factor, and residuals on a transect-integrated basis (middle), and physical plume age colored by the maleic anhydride (MA) to furan ratio (bottom). (b) Relative contribution of high-temperature factor for various wildfires obtained from this PMF (purple) and the two-factor PMF of the freshest plumes shown in Figure 1 (orange) on a transect-integrated basis. The numbers on purple bars show the average and standard deviation for all the transects of a specific fire.

represented photochemical aging. The following sections describe the best results for each of these PMF configurations.

Parameterizing Emissions. *Fresh Smoke Plume VOC Emissions Described by High- and Low-Temperature Pyrolysis Factors.* Total VOC mixing ratios are the highest in fresh biomass burning plumes and generally decrease after emission with aging and dilution during transport, as shown for the Williams Flats Fire on August 3rd, 2019 (Figure S1). The wildfire plumes contain various VOCs including long-lived (e.g., benzene), short-lived (e.g., furan), and species produced by chemical oxidation (i.e., secondary species, e.g., maleic anhydride).[42] The behavior of different VOCs varies from species to species and from plume to plume based on temporal evolution of emissions and spatial heterogeneity in atmospheric oxidation.[36,43,44] For example, mixing ratios of secondary species relative to short-lived species increase with plume age, as is shown by the ratio of maleic anhydride to furan (Figure S1). Maleic anhydride is a photochemical product of furan chemistry,[42] and the ratio can be used as a proxy for chemical plume age and thus to determine the freshest plume transects.[20] It should be noted that even for the freshest plumes selected here, significant aging had already occurred; for example, the physical age of the freshest plume transect for Williams Flats fire (00:39:23−00:44:44, August 4th, 2019) was 1.25 h.[20] In this section, we show that PMF analysis using the linear combination of the high- and low-temperature pyrolysis factors derived from FireLab measurements[34] can also be used to parameterize the composition of VOCs in fresh western US wildfire plumes.

https://doi.org/10.1021/acs.est.3c00537
Environ. Sci. Technol. 2023, 57, 13193−13204

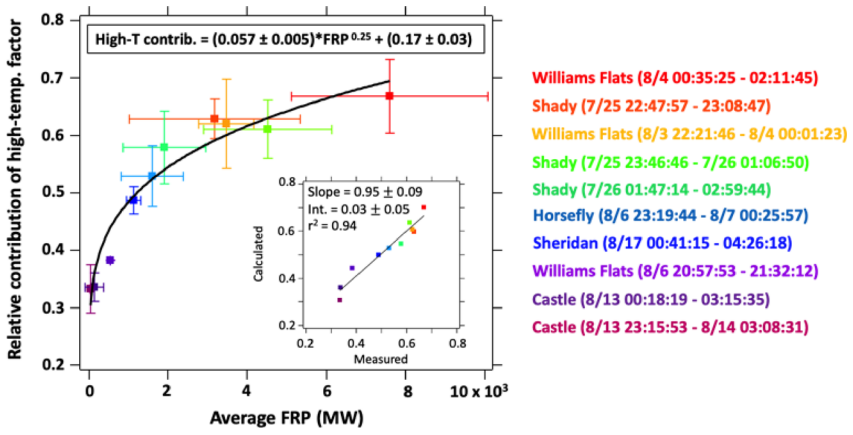

Figure 3. Scatter plot of the relative contribution of the high-temperature pyrolysis factor versus average FRP. Data are from 10 flights of 5 different fires with a total of 84 plume transects averaged per fire, where only plumes with less than 25% residual of the PMF fit were used. The colors represent different fires as shown in the right legend. The inset panel shows a linear fit of the PMF-determined high-temperature contribution versus the one calculated using the equation fitted by FRP. The scatter plot of the high-temperature factor versus FRP for individual plume transects is shown in Figure S3.

Figure 1a shows the PMF results of the freshest plume transects for 8 wildfires. The freshest plumes were determined by identifying transects from each fire where the physical plume age and maleic anhydride to furan ratio were the lowest. The two PMF factors were fully constrained by high- and low-temperature factors as determined from the FireLab data by Sekimoto et al.[34] Broadly, the total VOC emissions are described well, but the relative congtributions of the high- and low-temperature factors vary from fire to fire (Figure 1b). The sum of transect-integrated mixing ratios of all VOCs is used in Figure 1b. The residuals (i.e., the differences between the measured and calculated mixing ratios based on the PMF fits) are less than 25% for six of the fires (see blue bars in Figure 1b). Some of the fires with higher residuals were more aged (e.g., Williams Flats fire, August 9th), exhibited lower VOC mixing ratios (e.g., Tucker fire, Castle fire (00:26, August 13th), and Sheridan fire), or had unusual VOC compositions. For example, the Lick Creek fire was started on private lands and was a managed fire in a Grand fir-Douglas-fir forest that contained a lot of slash and logging piles,[35] which might have caused unusually high monoterpene emissions. Similar results were observed in the PMF analysis reported by Sekimoto et al.[34] for high monoterpene emitting fuels sampled during FireLab. Emissions of monoterpenes are driven by distillation processes, which are not well captured by the high- and low-temperature pyrolysis factors used here.

Long-Lived VOCs in Aged Smoke Described by High- and Low-Temperature Pyrolysis Factors. Chemical oxidation likely impacted PTR-ToF-MS measurements, even for the freshest plumes. Figure 1 shows that chemical oxidation was partly responsible for the residuals resulting from a fully constrained analysis of all 134 ions measued by PTR-ToF-MS, which includes masses that form downwind of fires (e.g., maleic anhydride). Mixing ratios of long-lived VOCs are more impacted by dilution than by chemistry and it can be expected that their relative ratios during transport will not change significantly from the emission ratios observed in fresh plumes. A two-factor PMF analysis was performed for all plumes and transects from the measured wildfires only using 22 long-lived VOCs, which includes species that have rate constants with OH radicals that are lower than benzene (1.2×10^{-12} cm^3/molecule/s) and have atmospheric lifetimes >50 days at OH $\sim 1.5 \times 10^6$ molecules/cm^3 (e.g., HCN, methanol, isocyanic acid, acetone, benzene, and butanedione, as shown in Table S2). We exclude secondary species from this analysis, as well as primary species with a low OH rate constant and significant secondary production (e.g., formic acid).

Figure 2 shows a two-factor PMF solution of the long-lived VOCs from transects of the Williams Flats Fire sampled over several hours of aging on two different days. This PMF run was fully constrained by the high- and low-temperature factors from Sekimoto et al.[34] For all plumes, the sum of the long-lived VOCs is described with residuals below 30%. The relative contribution of the high-temperature factor to the total resolved solution with the residual ignored (i.e., $\text{fraction}_{\text{high-temperature}}/(\text{fraction}_{\text{high-temperature}} + \text{fraction}_{\text{low-temperature}})$) is similar for most plume transects for each day (58 ± 10% for August 3rd and 67 ± 6% for August 4th). A higher residual is observed for transects where plumes are significantly more dilute. These higher residuals may result from the contributions of long-lived VOCs from background air. Despite this uncertainty, PMF analysis shows that the contribution of high- and low-temperature factors to the long-lived species across all transects is consistent with that observed from the freshest plume transect (Figure 2b). This supports the assumption that the ratios of long-lived species do not significantly change due to chemistry under the timescales considered here.

Figure 2 highlights results for a single fire. The detailed PMF results for the fires other than Williams Flats Fire (August 3rd−4th) are shown in Figure S2. The PMF solutions of the Tucker Fire, Ridge Top Fire, Mica and Lick Fire, and Williams Flats Fire (August 9th) had residuals higher than 35% for all plume transects because the plumes of those fires were significantly dilute, aged, or had unusual VOC composition (i.e., unusually high monoterpene emissions from the Lick slash and pile fire as described earlier) and were therefore excluded from this graph.

Parameterization of VOC Emissions with Fire Radiative Power. Fire radiative power (FRP) measured from satellites quantifies the rate of energy released from fires. FRP is often treated as a measure of biomass consumption and when combined with emission factors is used as a tool to estimate total VOC emissions.[45−49] The average FRP (in units of MW) was calculated for each plume transect as described by Stockwell et al.[36] First, the time since emission of the plume for each point in the transect was used to determine the FRP at the time of

https://doi.org/10.1021/acs.est.3c00537
Environ. Sci. Technol. 2023, 57, 13193−13204

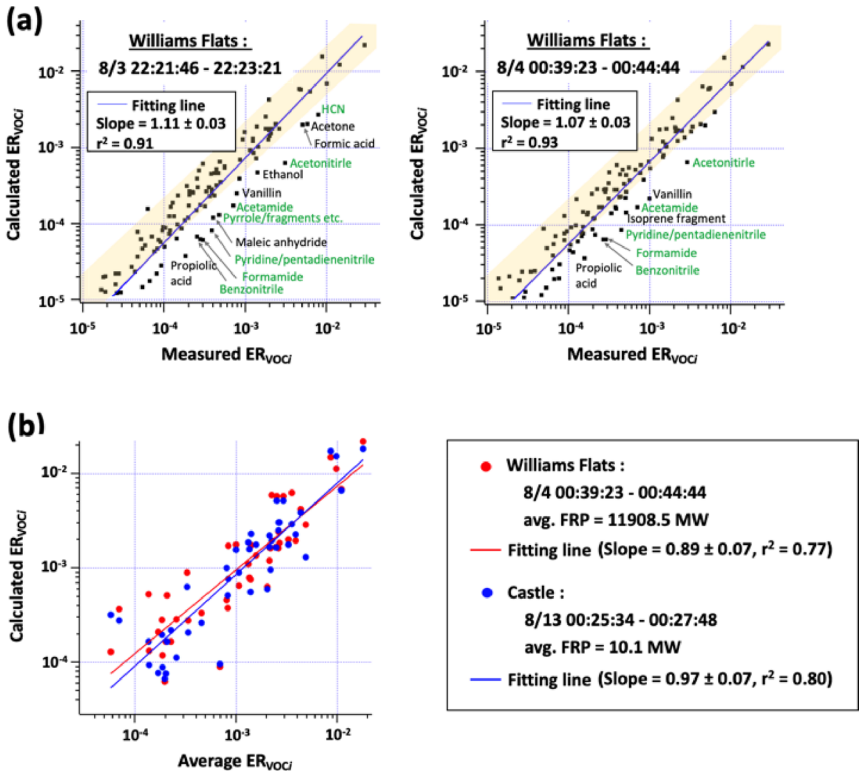

Figure 4. Comparison of emission ratios of VOC_i to CO (ER_{VOCi}): (a) Scatter plots of ER_{VOCi} calculated from average FRP and eq 6 versus measured ER_{VOCi} for the freshest plume transects of the Williams Flats fire (August 3rd and 4th, 2019). Data points correspond to 133 ion masses. The shaded area shows an uncertainty range of a factor of two (+100%/−50%). (b) Scatter plots of ER_{VOCi} calculated from average FRP and eq 6 for the freshest plume transects of Williams Flats (August 4th, 2019) and Castle fires (August 13th, 2019) versus average ERs from Gkatzelis et al.[20] Data points correspond to the 46 ion masses, which have been reported by Gkatzelis et al.[20] Slope and correlation coefficient (r^2) are obtained on a logarithmic scale. Results for other fires are shown in Figure S4.

emission. Then, the estimated instantaneous FRP was averaged over the time it took to complete an individual transect.

FRP values change with the size and the intensity of the fire, and it is expected that fires with higher FRP values often burn at higher temperatures, which will modulate the composition of the VOC emissions. Wooster et al. showed that the relationship between FRP and temperature (i.e., FRP ∝ temperature^4) is explained by the Stefan-Boltzmann law, which describes that the radiance and radiative divergence of a blackbody are proportional to the fourth power of its absolute temperature.[46] In Figure 3, the fire-averaged FRP is plotted versus the relative contribution of the high-temperature pyrolysis factor determined by the two-factor PMF analysis of the long-lived VOCs for various plumes that were described in Figure 2. Figure 3 shows that the relative contribution of the high-temperature pyrolysis factor is correlated with the average FRP based on the Stefan−Boltzmann law (i.e., high-temperature contribution ∝ FRP$^{0.25}$). With this relationship, FRP can therefore be used to estimate the relative amount of the high- and low-temperature pyrolysis factors, which can then be leveraged to determine the VOC composition of fresh emissions from satellite measurements.

In the following, the high- and low-temperature factors together with the fit equation from Figure 3 are used to estimate the emission ratios of the measured VOCs from fresh plumes of western US wildfires. Here, we focus on only fresh plumes, which means that the estimation requires only the high- and low-temperature factors, which are well defined from the FireLab measurements and this current study and do not include an aging factor, described further in Chemical Evolution of Short-Lived and Secondarily Produced VOCs.

According to the present PMF analysis, emissions of a given VOC in a fresh plume ("VOC_i" in units of ppbv) is calculated from the following equation:

$$\mathrm{VOC}_i\ [\mathrm{ppbv}] = \text{total VOCs [ppbv]} \times (a \times \text{high-}T_{\mathrm{VOC}i}\ [\mathrm{ppbv/total\ VOC\ ppbv}] + b \times \text{low-}T_{\mathrm{VOC}i}\ [\mathrm{ppbv/total\ VOC\ ppbv}]) \quad (1)$$

where "high-T_{VOCi}" and "low-T_{VOCi}" (ppbv/total VOC ppbv) are the relative fractions of the VOC_i-related ion mass to the total mass spectral profile for the high- and low-temperature pyrolysis factors, respectively (shown in Table S1b). "Total VOCs" represents the sum of transect-integrated emissions (in units of ppbv) of all VOCs. Coefficient "a" corresponds to the relative contribution of the high-temperature factor and thus can be determined from the average FRP of the corresponding plume and the fitting function as shown in Figure 3, i.e.,

$$a = 0.057 \times \text{average FRP [MW]}^{0.25} + 0.17 \quad (2)$$

Coefficient "b" is the relative contribution of the low-temperature factor. Thus,

$$b = 1 - a \quad (3)$$

Gkatzelis et al.[20] showed that that total VOC emissions in fresh plumes measured during FIREX-AQ are well correlated with carbon monoxide (CO) emissions:

https://doi.org/10.1021/acs.est.3c00537
Environ. Sci. Technol. 2023, 57, 13193−13204

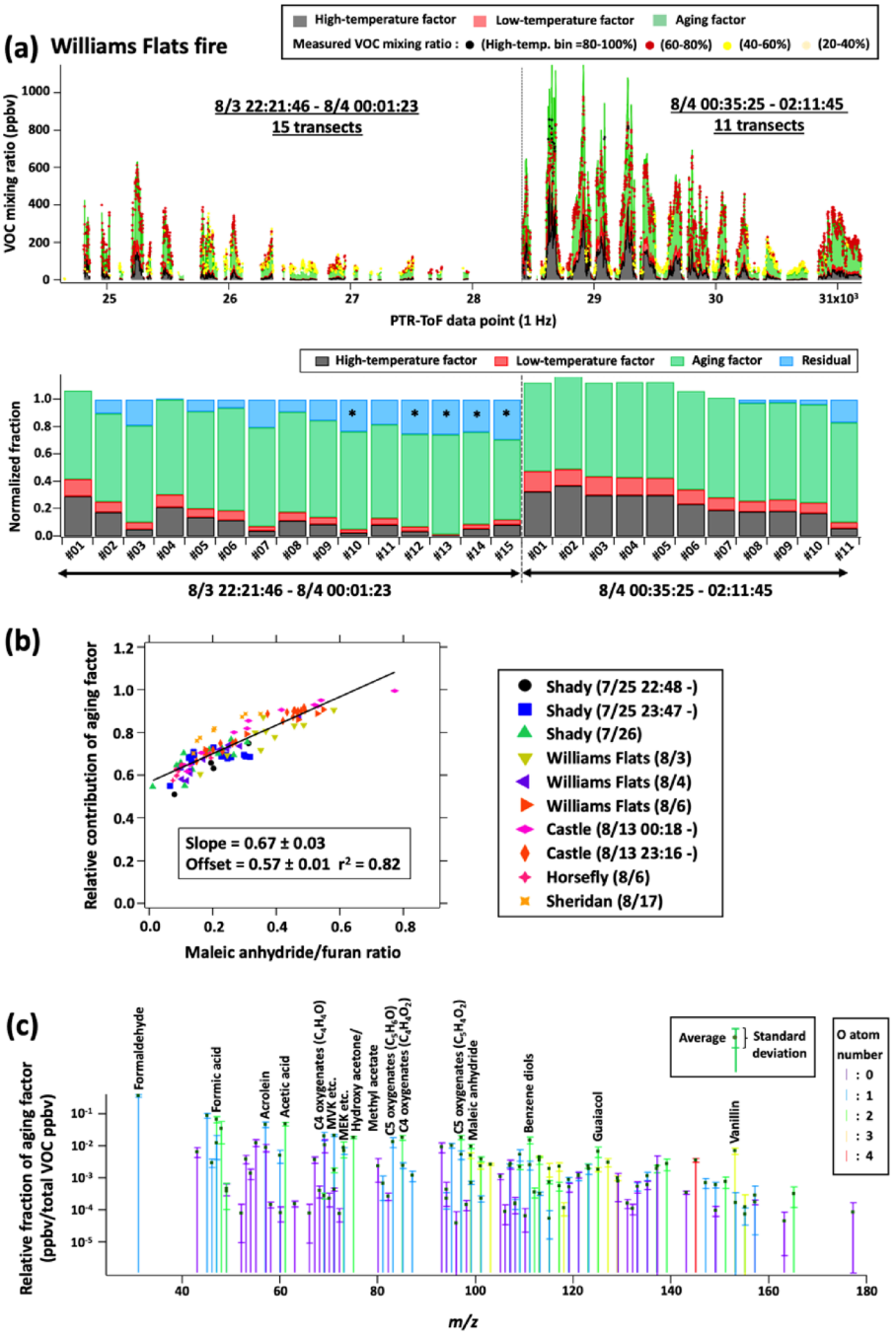

Figure 5. Three-factor PMF solutions fully constrained by high- and low-temperature pyrolysis factors, for short-lived and secondarily produced VOCs. PMF was separately performed on five bins of high-temperature factor contributions. (a) Results for Williams Flats fire (August 3rd and 4th, 2019): the sum of the PTR-ToF-MS-measured total VOC mixing ratios and PMF fits (upper panel), and transect-integrated fractions of the high-temperature factor, low-temperature factor, aging factor, and residual (lower panel). There were no data for the high-temperature bin = 0−20% in these plume transects. The asterisk in the lower panel means that residuals were higher than 20%. Fractions >1 means that the PMF solutions were larger than the measurements. Results for other fires are shown in Figure S5. (b) Scatter plot of the relative contribution of the aging factor versus the maleic anhydride to furan ratio. (c) Average VOC emission profiles of the aging factor obtained from PMF of different high-temperature contribution categories. Colors indicate the oxygen atom number included in the VOCs. PMF results of the high-temperature factor contribution of 0−20% have large residuals, and the corresponding profile was excluded. Fractions of individual ions are shown in Table S1c.

$$\text{total VOCs [ppbv]} = (0.127 \pm 0.004) \times \text{CO [ppbv]} + (11.29 \pm 9.4) \quad (4)$$

The ratio of total VOCs to CO (i.e., Total VOCs [ppbv]/CO [ppbv]) can be approximated to 0.127, as the intercept of eq 4 is small and negligible.

$$\frac{\text{total VOCs [ppbv]}}{\text{CO [ppbv]}} \approx 0.127 \quad (5)$$

Consequently, according to eqs 1−5, the emission ratio of VOC_i to CO, ER_{VOCi}, can be estimated just from FRP measurements as well as the following equation:

https://doi.org/10.1021/acs.est.3c00537
Environ. Sci. Technol. 2023, 57, 13193−13204

$$\begin{aligned}\mathrm{ERVOC}i &= \frac{\mathrm{VOC}_i\ [\mathrm{ppbv}]}{\mathrm{CO}\ [\mathrm{ppbv}]} \\ &= 0.127 \times \{(0.057 \times \text{average FRP [MW]}0.25 \\ &\quad + 0.17) \\ &\times \text{high-}T_{\mathrm{VOC}i}\ [\text{ppbv/total VOC ppbv}] \\ &\quad + (0.83 - 0.057 \times \text{average FRP [MW]}^{0.25}) \\ &\times \text{low-}T_{\mathrm{VOC}i}\ [\text{ppbv/total VOC ppbv}]\}\end{aligned} \quad (6)$$

We discuss how accurately ER_{VOCi} is calculated from average FRP and eq 6 by comparing with the measured ERs (determined here for the 134 ion masses used in the PMF). Figure 4a shows the scatter plots of the calculated ER_{VOCi} versus the measured ones for the freshest plume transects of the Williams Flats Fire. The measured ER_{VOCi} was obtained from transect-integrated emissions of individual VOC_i and CO. The agreement between the measured and calculated ER_{VOCi} has a slope of ∼1.1 and r^2 > 0.90. The calculated ER_{VOCi} of approximately 90 VOCs were within a factor of two (+100%/−50%). However, specific VOCs denoted in Figure 4a, mainly nitrogen-containing species (such as nitriles and amides) and some oxygenates, are likely underestimated. This could be caused by the fuel nitrogen content adding additional variability to the nitrogen-containing VOC emissions.[50,51] Similar results were observed for other fires (Figure S4a). Only $[C_2H_6S + H]^+$ assigned as dimethyl sulfide was excluded because the calculated and measured ERs were too low to be fitted properly.

Figure 4b compares the Williams Flats Fire, which had the highest average FRP of the freshest plume transect (∼12,000 MW), with the Castle fire, which had the lowest FRP (∼10 MW). The data used here are average ERs from the freshest wildfire plume transects sampled during the FIREX-AQ taken from Gkatzelis et al.[20] That study only includes 46 masses that were clearly identified, while we use all compounds with significant signals in this study. The 46 masses account for more than 85% of the total 134 VOC emissions used in this study. The fits between the calculated and average ER_{VOCi} are similar with slopes of 0.89 and 0.97 and r^2 = 0.77 and 0.80, respectively. Other fires were also similar (Figure S4b). This shows that satellite-derived FRP together with the high- and low-temperature factors can be used to estimate VOC emission ratios independent of fuel type and burning condition.

Chemical Evolution of Short-Lived and Secondarily Produced VOCs. The VOC profile of each fire plume evolves downwind with photochemical aging. In addition, the VOC composition in each plume transect will depend upon the original composition of the fresh plume, which is described by the high- and low-temperature profiles as discussed above. As a result, the high- and low-temperature factors alone cannot describe the short-lived and secondarily produced VOCs in downwind plumes and transects. A third factor, interpreted as an "aging factor", has to be added to fit the VOC distribution as the plume advects downwind.

Figure 5 shows the results of a three-factor PMF solution for only the short-lived and secondarily produced VOCs. In order to control for differences in starting VOC composition in each plume, the time series data were first separated into five bins with varying high-temperature factor contributions: 0−20, 20−40, 40−60, 60−80, and 80−100% as obtained from the two-factor solution of the long-lived VOCs. To reflect the VOC compositions of the fresh emissions, the ratio between the high- and low-temperature factors were held constant in each bin (e.g., in the case of the bin of 80−100% high-temperature contribution, the ratio between the high- and low-temperature factors were held constant at 90 and 10%). PMF was performed separately on each bin, and the two factors were fully constrained by the high- and low-temperature factors.[34] One unconstrained factor (referred to as "aging factor") was included to be optimized by PMF. We analyze the data in this way in order to resolve differences in the atmospheric chemistry and production of secondary VOCs of the high-temperature pyrolysis products (e.g., aromatics) from that of the low-temperature pyrolysis products (e.g., phenolics, furans). The sum of PTR-ToF-MS-measured total VOC mixing ratios and the PMF fits were then reordered to the original time series, and normalized fractions of each factor and residuals were calculated on a transect-integrated basis. For PMF solutions with four or more factors, additional factors were a combination of the three factors and did not provide additional insight into the data.

Figure 5a shows the results of this PMF analysis for the same plumes and transects from the Williams Flats Fire as in Figure 2. The short-lived and secondarily produced VOCs are well-fit with low residuals (<30%) for most transects. The assignment of the third factor as "aging factor" was based on (1) the relative contribution of this factor increasing with plume age and (2) the good correlation of this factor's contribution with the maleic anhydride to furan ratio (Figure 5b). These results indicate that a higher contribution of the aging factor results from prolonged photochemistry. The assignment is further supported by the VOC composition of the aging factor, which is shown in Figure 5c. The aging factor is mostly comprised of oxygenated species: small carbonyls such as formaldehyde and acetaldehyde, small acids such as formic acid and acetic acid, and various C4 and C5 oxygenates. These compounds are often secondary species observed in air masses that have undergone atmospheric oxidation, and chamber experiments of wildfire smoke showed similar increases of these compounds with photochemical aging.[42,52] Furthermore, the distribution of these VOCs and evolution downwind appears similar regardless of the starting VOC composition, i.e., there are no significant differences in the PMF solutions for each of the high-temperature bins. This result is also consistent with laboratory experiments, which showed that PTR-ToF-MS spectra of aged smoke is not significantly different for fires that contain significant amounts of low-temperature pyrolysis products vs those that have significant amounts of high-temperature pyrolysis products.[42,52]

It should be noted that the short-lived and secondary compounds in the freshest plumes (e.g., transect #01 in Figure 5a) already have large contributions of the aging factor (∼60%), while fresh plumes and long-lived species can be well described with only the high- and low-temperature factors as shown in Figure 1a. This difference is partly explained by rapid photochemistry in biomass burning plumes, which can quickly alter smoke in the minutes to hour timeframe before the DC-8 sampled the fire plumes.[43,53] It should be mentioned that PMF was not able to separate out an aging factor for the very freshest plumes, such as observed in the FireLab[34] or from fresh near-field VOC emissions collected by ground-site sampling during the FIREX-AQ project.[54] Another reason is that the small oxygenated VOCs are also primary emissions that are significant in the high- and low-temperature factors and PMF assigns some of them to the aging factor as well in the fresh plumes. But again, it should be mentioned that the high- and low-temperature

https://doi.org/10.1021/acs.est.3c00537
Environ. Sci. Technol. 2023, 57, 13193−13204

pyrolysis factors alone can adequately account for the freshest wildfire plumes.

Implication and Perspective on Atmospheric Sciences. This work focused on understanding VOC emissions in fresh plumes from western US wildfires by using the high- and low-temperature pyrolysis factors that were obtained in the FireLab measurements.[34] Even though the wildfires measured during FIREX-AQ varied significantly in fuel composition, fire processes, and fire size and intensity, the presented PMF analysis described the VOC emissions from individual wildfires well with the two factors. In addition, the relative contribution of the two factors was dependent on FRP measured by satellite. This shows that the VOC variability in fresh wildfire plumes is more determined by the fire temperature and the resulting pyrolysis processes than the fuel type.

Based on these results, we provide a new framework to estimate VOC/CO emission ratios from western US wildfires for many VOCs (>100 species) that only relies on FRP measurements from satellites and the high- and low-temperature pyrolysis profiles published in this and previous laboratory work. Many total carbon fire emission calculations already rely primarily on FRP[36] and with this approach as presented here the VOC composition could also be simply but effectively parameterized in models without knowing the MCE for each fire.

■ ASSOCIATED CONTENT

Supporting Information

The Supporting Information is available free of charge at https://pubs.acs.org/doi/10.1021/acs.est.3c00537.

Results of additional fires not shown in the main text, PMF configurations, and descriptions on preparation of datasets for PMF analysis (, and Figures S1−S16) (PDF)

Information of 134 PTR-ToF-MS ion masses, relative fractions and standard deviation of mass spectral profiles for high- and low-temperature pyrolysis factors used in the present PMF analysis, and average and standard deviation of relative fractions of aging factor obtained in this study (XLSX)

■ AUTHOR INFORMATION

Corresponding Author

Kanako Sekimoto − *Graduate School of Nanobioscience, Yokohama City University, Yokohama, Kanagawa 236-0027, Japan;* orcid.org/0000-0001-9908-9698; Email: sekimoto@yokohama-cu.ac.jp

Authors

Matthew M. Coggon − *NOAA Chemical Sciences Laboratory, Boulder, Corolado 80305, United States;* orcid.org/0000-0002-5763-1925

Georgios I. Gkatzelis − *NOAA Chemical Sciences Laboratory, Boulder, Corolado 80305, United States; Cooperative Institute for Research in Environmental Sciences, University of Colorado Boulder, Boulder, Colorado 80309, United States;* Present Address: Institute of Energy and Climate Research, IEK-8: Troposphere, Forschungszentrum Jülich GmbH, Jülich 52428, Germany.; orcid.org/0000-0002-4608-3695

Chelsea E. Stockwell − *NOAA Chemical Sciences Laboratory, Boulder, Corolado 80305, United States; Cooperative Institute for Research in Environmental Sciences, University of Colorado Boulder, Boulder, Colorado 80309, United States;* orcid.org/0000-0003-3462-2126

Jeff Peischl − *NOAA Chemical Sciences Laboratory, Boulder, Corolado 80305, United States; Cooperative Institute for Research in Environmental Sciences, University of Colorado Boulder, Boulder, Colorado 80309, United States;* orcid.org/0000-0002-9320-7101

Amber J. Soja − *National Institute of Aerospace, Hampton, Virginia 23666, United States; NASA Langley Research Center, Hampton, Virginia 23681, United States;* orcid.org/0000-0001-8637-3040

Carsten Warneke − *NOAA Chemical Sciences Laboratory, Boulder, Corolado 80305, United States;* orcid.org/0000-0003-3811-8496

Complete contact information is available at: https://pubs.acs.org/10.1021/acs.est.3c00537

Notes

The authors declare no competing financial interest.

■ ACKNOWLEDGMENTS

We would like to thank the NASA/NOAA FIREX-AQ science and aircraft operation teams. K.S. acknowledges the Post-doctoral Fellowships for Research Abroad from the Japan Society for the Promotion of Science (JSPS) and a Grant-in-Aid for Scientific Research (C) (JP21K12223) from the Ministry of Education, Culture, Sports, Science and Technology of Japan. This research was supported in part by NOAA cooperative agreements NA17OAR4320101 and NA22OAR4320151.

■ REFERENCES

(1) Jaffe, D. A.; O'Neill, S. M.; Larkin, N. K.; Holder, A. L.; Peterson, D. L.; Halofsky, J. E.; Rappold, A. G. Wildfire and prescribed burning impacts on air quality in the United States. *J. Air Waste Manag. Assoc.* **2020**, *70*, 583−615.

(2) O'Dell, K.; Ford, B.; Fischer, E. V.; Pierce, J. R. Contribution of Wildland-Fire Smoke to US PM. *Environ. Sci. Technol.* **2019**, *53*, 1797−1804.

(3) Wotawa, G.; Trainer, M. The influence of Canadian forest fires on pollutant concentrations in the United states. *Science* **2000**, *288*, 324−328.

(4) Johnston, F. H.; Henderson, S. B.; Chen, Y.; Randerson, J. T.; Marlier, M.; Defries, R. S.; Kinney, P.; Bowman, D. M.; Brauer, M. Estimated global mortality attributable to smoke from landscape fires. *Environ. Health Perspect.* **2012**, *120*, 695−701.

(5) Johnston, F. H.; Borchers-Arriagada, N.; Morgan, G. G.; Jalaludin, B.; Palmer, A. J.; Williamson, G. J.; Bowman, D. M. J. S. Unprecedented health costs of smoke-related PM 2.5 from the 2019−20 Australian megafires. *Nat. Sustainability* **2021**, *4*, 42−47.

(6) Burke, M.; Driscoll, A.; Heft-Neal, S.; Xue, J.; Burney, J.; Wara, M. The changing risk and burden of wildfire in the United States. *Proc. Natl. Acad. Sci. U. S. A.Proc Natl Acad Sci U S A* **2021**, *118*, No. e2011048118.

(7) Westerling, A. L. Increasing western US forest wildfire activity: sensitivity to changes in the timing of spring. *Philos Trans R Soc Lond B* **2016**, *371*, 20150178.

(8) Alvarado, M. J.; Wang, C.; Prinn, R. G. Formation of ozone and growth of aerosols in young smoke plumes from biomass burning: 2. Three-dimensional Eulerian studies. *J. Geophys. Res. Atmos.* **2009**, *114*, D09307.

(9) Alvarado, M. J.; Lonsdale, C. R.; Yokelson, R. J.; Akagi, S. K.; Coe, H.; Craven, J. S.; Fischer, E. V.; McMeeking, G. R.; Seinfeld, J. H.; Soni, T.; Taylor, J. W.; Weise, D. R.; Wold, C. E. Investigating the links between ozone and organic aerosol chemistry in a biomass burning

plume from a prescribed fire in California chaparral. *Atmos. Chem. Phys.* **2015**, *15*, 6667−6688.
(10) Yokelson, R. J.; Crounse, J. D.; DeCarlo, P. F.; Karl, T.; Urbanski, S.; Atlas, E.; Campos, T.; Shinozuka, Y.; Kapustin, V.; Clarke, A. D.; Weinheimer, A.; Knapp, D. J.; Montzka, D. D.; Holloway, J.; Weibring, P.; Flocke, F.; Zheng, W.; Toohey, D.; Wennberg, P. O.; Wiedinmyer, C.; Mauldin, L.; Fried, A.; Richter, D.; Walega, J.; Jimenez, J. L.; Adachi, K.; Buseck, P. R.; Hall, S. R.; Shetter, R. Emissions from biomass burning in the Yucatan. *Atmos. Chem. Phys.* **2009**, *9*, 5785−5812.
(11) Jaffe, D. A.; Wigder, N. L. Ozone production from wildfires: A critical review. *Atmos. Environ.* **2012**, *51*, 1−10.
(12) Naeher, L. P.; Brauer, M.; Lipsett, M.; Zelikoff, J. T.; Simpson, C. D.; Koenig, J. Q.; Smith, K. R. Woodsmoke health effects: a review. *Inhalation Toxicol.* **2007**, *19*, 67−106.
(13) Roberts, J. M.; Veres, P. R.; Cochran, A. K.; Warneke, C.; Burling, I. R.; Yokelson, R. J.; Lerner, B.; Gilman, J. B.; Kuster, W. C.; Fall, R.; de Gouw, J. Isocyanic acid in the atmosphere and its possible link to smoke-related health effects. *Proc. Natl. Acad. Sci. U. S. A.* **2011**, *108*, 8966−8971.
(14) Mouat, A. P.; Paton-Walsh, C.; Simmons, J. B.; Ramirez-Gamboa, J.; Griffith, D. W. T.; Kaiser, J. Emission factors of long-lived volatile organic compounds from the 2019−2020 Australian wildfires during the COALA campaign. *Atmos. Chem. Phys. Discuss* **2022**, *22*, 11033−11047.
(15) Stockwell, C. E.; Jayarathne, T.; Cochrane, M. A.; Ryan, K. C.; Putra, E. I.; Saharjo, B. H.; Nurhayati, A. D.; Albar, I.; Blake, D. R.; Simpson, I. J.; Stone, E. A.; Yokelson, R. J. Field measurements of trace gases and aerosols emitted by peat fires in Central Kalimantan, Indonesia, during the 2015 El Niño. *Atmos. Chem. Phys.* **2016**, *16*, 11711−11732.
(16) Lindaas, J.; Pollack, I. B.; Garofalo, L. A.; Pothier, M. A.; Farmer, D. K.; Kreidenweis, S. M.; Campos, T. L.; Flocke, F.; Weinheimer, A. J.; Montzka, D. D.; Tyndall, G. S.; Palm, B. B.; Peng, Q.; Thornton, J. A.; Permar, W.; Wielgasz, C.; Hu, L.; Ottmar, R. D.; Restaino, J. C.; Hudak, A. T.; Ku, I.-T.; Zhou, Y.; Sive, B. C.; Sullivan, A.; Collett, J. L., Jr.; Fischer, E. V. Emissions of Reactive Nitrogen From Western U.S. Wildfires During Summer 2018. *J. Geophys. Res. Atmos.* **2021**, *126*, No. e2020JD032657.
(17) Peng, Q.; Palm, B. B.; Melander, K. E.; Lee, B. H.; Hall, S. R.; Ullmann, K.; Campos, T.; Weinheimer, A. J.; Apel, E. C.; Hornbrook, R. S.; Hills, A. J.; Montzka, D. D.; Flocke, F.; Hu, L.; Permar, W.; Wielgasz, C.; Lindaas, J.; Pollack, I. B.; Fischer, E. V.; Bertram, T. H.; Thornton, J. A. HONO Emissions from Western U. S. Wildfires Provide Dominant Radical Source in Fresh Wildfire Smoke. *Environ. Sci. Technol.* **2020**, *54*, 5954−5963.
(18) Permar, W.; Wang, Q.; Selimovic, V.; Wielgasz, C.; Yokelson, R. J.; Hornbrook, R. S.; Hills, A. J.; Apel, E. C.; Ku, I.-T.; Zhou, Y.; Siva, B. C.; Sullivan, A. P.; Collett, J. L., Jr.; Campos, T. L.; Palm, B. B.; Peng, Q.; Thornton, J. A.; Garofalo, L. A.; Farmer, D. K.; Kreidenweis, S. M.; Levin, E. J. T.; DeMott, P. J.; Flocke, F.; Fischer, E. V.; Hu, L. Emissions of Trace Organic Gases From Western U.S. Wildfires Based on WE-CAN Aircraft Measurements. *J. Geophys. Res. Atmos.* **2021**, *126*, No. e2020JD033838.
(19) Liu, X.; Huey, L. G.; Yokelson, R. J.; Selimovic, V.; Simpson, I. J.; Müller, M.; Jimenez, J. L.; Campuzano-Jost, P.; Beyersdorf, A. J.; Blake, D. R.; Butterfield, Z.; Choi, Y.; Crounse, J. D.; Day, D. A.; Diskin, G. S.; Dubey, M. K.; Fortner, E.; Hanisco, T. F.; Hu, W.; King, L. E.; Kleinman, L.; Meinardi, S.; Mikoviny, T.; Onasch, T. B.; Palm, B. B.; Peischl, J.; Pollack, I. B.; Ryerson, T. B.; Sachse, G. W.; Sedlacek, A. J.; Shilling, J. E.; Springston, S.; Clair, J. M.; Tanner, D. J.; Teng, A. P.; Wennberg, P. O.; Wisthaler, A.; Wolfe, G. M. Airborne measurements of western U.S. wildfire emissions: Comparison with prescribed burning and air quality implications. *J. Geophys Res Atmos* **2017**, *122*, 6108−6129.
(20) Gkatzelis, G. I.; Coggon, M. M.; Stockwell, C. E.; Hornbrook, R. S.; Allen, H.; Apel, E. C.; Bela, M. M.; Blake, D. R.; Bourgeois, I.; Brown, S. S.; Campuzano-Jost, P.; St. Clair, J. M.; Crauford, J. H.; Crounse, J. D.; Day, D. A.; DiGangi, J. P.; Diskin, G. S.; Fried, A.; Gilman, J. B.; Guo, H.; Hair, J. W.; Halliday, H. S.; Hanisco, T. F.; Hannun, R.; Hills, A.; Huey, L. G.; Jimenez, J. L.; Katich, J. M.; Lamplugh, A.; Ro Lee, Y.; Liao, J.; Lindaas, J.; McKeen, S. A.; Mikoviny, T.; Nault, B. A.; Neuman, J. A.; Nowak, J. B.; Pagonis, D.; Peischl, J.; Perring, A. E.; Piel, F.; Rickly, P. S.; Robinson, M. A.; Rollins, A. W.; Ryerson, T. B.; Schueneman, M. K.; Schwantes, R. H.; Schwarz, J. P.; Sekimoto, K.; Selimovic, V.; Shingler, T.; Tanner, D. J.; Tomsche, L.; Vasquez, K. T.; Veres, P. R.; Washenfelder, R.; Weibring, P.; Wennberg, P. O.; Wisthaler, A.; Wolfe, G. M.; Womack, C. C.; Xu, L.; Yokelson, R. J.; Warneke, C. Parameterization of US wildfire and prescribed fire emission ratios and emission factors based on FIREX-AQ aircraft measurements. *EGUsphere* **2023**, 1.
(21) Koss, A. R.; Sekimoto, K.; Gilman, J. B.; Selimovic, V.; Coggon, M. M.; Zarzana, K. J.; Yuan, B.; Lerner, B. M.; Brown, S. S.; Jimenez, J. L.; Krechmer, J.; Roberts, J. M.; Warneke, C.; Yokelson, R. J.; de Gouw, J. Non-methane organic gas emissions from biomass burning: identification, quantification, and emission factors from PTR-ToF during the FIREX 2016 laboratory experiment. *Atmos. Chem. Phys.* **2018**, *18*, 3299−3319.
(22) Selimovic, V.; Yokelson, R. J.; Warneke, C.; Roberts, J. M.; de Gouw, J.; Reardon, J.; Griffith, D. W. T. Aerosol optical properties and trace gas emissions by PAX and OP-FTIR for laboratory-simulated western US wildfires during FIREX. *Atmos. Chem. Phys.* **2018**, *18*, 2929−2948.
(23) Stockwell, C. E.; Yokelson, R. J.; Kreidenweis, S. M.; Robinson, A. L.; DeMott, P. J.; Sullivan, R. C.; Reardon, J.; Ryan, K. C.; Griffith, D. W. T.; Stevens, L. Trace gas emissions from combustion of peat, crop residue, domestic biofuels, grasses, and other fuels: configuration and Fourier transform infrared (FTIR) component of the fourth Fire Lab at Missoula Experiment (FLAME-4). *Atmos. Chem. Phys.* **2014**, *14*, 9727−9754.
(24) Akagi, S. K.; Yokelson, R. J.; Wiedinmyer, C.; Alvarado, M. J.; Reid, J. S.; Karl, T.; Crounse, J. D.; Wennberg, P. O. Emission factors for open and domestic biomass burning for use in atmospheric models. *Atmos. Chem. Phys.* **2011**, *11*, 4039−4072.
(25) Andreae, M. O.; Merlet, P. Emission of trace gases and aerosols from biomass burning. *Global Biogeochem. Cycles* **2001**, *15*, 955−966.
(26) Andreae, M. O. Emission of trace gases and aerosols from biomass burning − an updated assessment. *Atmos. Chem. Phys.* **2019**, *19*, 8523−8546.
(27) Warneke, C.; Roberts, J. M.; Veres, P.; Gilman, J.; Kuster, W. C.; Burling, I.; Yokelson, R.; de Gouw, J. A. VOC identification and inter-comparison from laboratory biomass burning using PTR-MS and PIT-MS. *Int. J. Mass Spectrom.* **2011**, *303*, 6−14.
(28) Yokelson, R. J.; Burling, I. R.; Gilman, J. B.; Warneke, C.; Stockwell, C. E.; de Gouw, J.; Akagi, S. K.; Urbanski, S. P.; Veres, P.; Roberts, J. M.; Kuster, W. C.; Reardon, J.; Griffith, D. W. T.; Johnson, T. J.; Hosseini, S.; Miller, J. W.; Cocker, D. R., III; Jung, H.; Weise, D. R. Coupling field and laboratory measurements to estimate the emission factors of identified and unidentified trace gases for prescribed fires. *Atmos. Chem. Phys.* **2013**, *13*, 89−116.
(29) Hatch, L. E.; Yokelson, R. J.; Stockwell, C. E.; Veres, P. R.; Simpson, I. J.; Blake, D. R.; Orlando, J. J.; Barsanti, K. C. Multi-instrument comparison and compilation of non-methane organic gas emissions from biomass burning and implications for smoke-derived secondary organic aerosol precursors. *Atmos. Chem. Phys.* **2017**, *17*, 1471−1489.
(30) Yokelson, R. J.; Griffith, D. W. T.; Ward, D. E. Open-path Fourier transform infrared studies of large-scale laboratory biomass fires. *J. Geophys. Res. Atmos.* **1996**, *101*, 21067−21080.
(31) Yokelson, R. J.; Susott, R.; Ward, D. E.; Reardon, J.; Griffith, D. W. T. Emissions from smoldering combustion of biomass measured by open-path Fourier transform infrared spectroscopy. *J. Geophys. Res. Atmos.* **1997**, *102*, 18865−18877.
(32) Collard, F. -X.; Blin, J. A review on pyrolysis of biomass constituents: Mechanisms and composition of the products obtained from the conversion of cellulose, hemicelluloses and lignin. *Renewable Sustainainable Energy Rev.* **2014**, *38*, 594−608.

(33) Liu, W. J.; Li, W. W.; Jiang, H.; Yu, H. Q. Fates of Chemical Elements in Biomass during Its Pyrolysis. *Chem. Rev.* **2017**, *117*, 6367−6398.
(34) Sekimoto, K.; Koss, A. R.; Gilman, J. B.; Selimovic, V.; Coggon, M. M.; Zarzana, K. J.; Yuan, B.; Lerner, B. M.; Brown, S. S.; Warneke, C.; Yokelson, R. J.; Roberts, J. M.; de Gouw, J. High- and low-temperature pyrolysis profiles describe volatile organic compound emissions from western US wildfire fuels. *Atmos. Chem. Phys.* **2018**, *18*, 9263−9281.
(35) Warneke, C.; Schwarz, J. P.; Dibb, J.; Kalashnikova, O.; Frost, G.; Al-Saad, J.; Brown, S. S.; Brewer, W. A.; Soja, A.; Seidel, F. C.; Washenfelder, R. A.; Wiggins, E. B.; Moore, R. H.; Anderson, B. E.; Jordan, C.; Yaclvitch, T. I.; Herndon, S. C.; Liu, S.; Kuwayama, T.; Jaffe, D.; Johnson, N.; Selimovic, V.; Yokelson, R.; Giles, D. M.; Holben, B. N.; Goloub, P.; Popovici, I.; Trainer, M.; Kumar, A.; Pierce, B.; Fahey, D.; Roberts, J.; Gargulinski, E. M.; Peterson, D. A.; Ye, X.; Thapa, L. H.; Saide, P. E.; Fite, C. H.; Holmes, C. D.; Wang, S.; Coggon, M. M.; Decker, Z. C. J.; Stockwell, C. E.; Xu, L.; Gkatzelis, G.; Aikin, K.; Llefer, B.; Kaspari, J.; Griffin, D.; Zeng, L.; Weber, R.; Hastings, M.; Chai, J.; Wolfe, G. M.; Hanisco, T. F.; Liao, J.; Jost, P. C.; Guo, H.; Jimenez, J. L.; Crawford, J. The FIREX-AQ Science Team. Fire Influence on Regional to Global Environments and Air Quality (FIREX-AQ). *J. Geophys. Res. Atmos.* **2023**, *128*, No. e2022JD037758.
(36) Stockwell, C. E.; Bela, M. M.; Coggon, M. M.; Gkatzelis, G. I.; Wiggins, E.; Gargulinski, E. M.; Shingler, T.; Fenn, M.; Griffin, D.; Holmes, C. D.; Ye, X.; Saide, P. E.; Bourgeois, I.; Peischl, J.; Womack, C. C.; Washenfelder, R. A.; Veres, P. R.; Neuman, J. A.; Gilman, J. B.; Lamplugh, A.; Schwantes, R. H.; McKeen, S. A.; Wisthaler, A.; Piel, F.; Guo, H.; Campuzano-Jost, P.; Jimenez, J. L.; Fried, A.; Hanisco, T. F.; Huey, L. G.; Perring, A.; Katich, J. M.; Diskin, G. S.; Nowak, J. B.; Bui, Y. P.; Halliday, H. S.; DiGangi, J. P.; Pereria, G.; James, E. P.; Ahmadov, R.; McLinden, C. A.; Soja, A. J.; Moore, R. H.; Hair, J. W.; Warneke, C. Airborne Emission Rate Measurements Validate Remote Sensing Observations and Emission Inventories of Western U.S Wildfires. *Environ. Sci. Technol.* **2022**, *56*, 7564−7577.
(37) Schmidt, C. Chapter 13-Monitoring fires with the GOES-R series. In *The GOES-R series: A new generation of geostationary environmental satellites*, Elsevier, 2020; pp. 145−163.
(38) Wiggins, E. B.; Soja, A. J.; Gargulinski, E.; Halliday, H. S.; Pierce, R. B.; Schmidt, C. C.; Nowak, J. B.; DiGangi, J. P.; Diskin, G. S.; Katich, J. M.; Perring, A. E.; Schwarz, J. P.; Anderson, B. E.; Chen, G.; Crosbie, E. C.; Jordan, C.; Robinson, C. E.; Sanchez, K. J.; Shingler, T. J.; Shook, M.; Thornhill, K. L.; Winstead, E. L.; Ziemba, L. D.; Moore, R. H. High Temporal Resolution Satellite Observations of Fire Radiative Power Reveal Link Between Fire Behavior and Aerosol and Gas Emissions. *Geophys. Res. Lett.* **2020**, *47*, No. e2020GL090707.
(39) Bourgeois, I.; Peischl, J.; Neuman, J. A.; Brown, S. S.; Allen, H. M.; Campuzano-Jost, P.; Coggon, M. M.; DiGangi, J. P.; Diskin, G. S.; Gilman, J. B.; Gkatzelis, G. I.; Guo, H.; Halliday, H. A.; Hanisco, T. F.; Holmes, C. D.; Huey, L. G.; Jimenez, J. L.; Lamplugh, A. D.; Lee, Y. R.; Lindaas, J.; Moore, R. H.; Nault, B. A.; Nowak, J. B.; Pagonis, D.; Rickly, P. S.; Robinson, M. A.; Rollins, A. W.; Selimovic, V.; St. Clair, J. M.; Tanner, D.; Vasquez, K. T.; Veres, P. R.; Warneke, C.; Wennberg, P. O.; Washenfelder, R. A.; Wiggins, E. B.; Womack, C. C.; Xu, L.; Zarzana, K. J.; Ryerson, T. B. Comparison of airborne measurements of NO, NO_2, HONO, NO_y, and CO during FIREX-AQ. *Atmos. Meas. Technol.* **2022**, *15*, 4901−4930.
(40) Canonaco, F.; Crippa, M.; Slowik, J. G.; Baltensperger, U.; Prévôt, A. S. H. SoFi, an IGOR-based interface for the efficient use of the generalized multilinear engine (ME-2) for the source apportionment: ME-2 application to aerosol mass spectrometer data. *Atmos. Meas Technol.* **2013**, *6*, 3649−3661.
(41) Paatero, P. The Multilinear Engine—A Table-Driven, Least Squares Program for Solving Multilinear Problems, Including the n-Way Parallel Factor Analysis Model. *J. Comput. Graph Stat* **1999**, *8*, 854−888.
(42) Coggon, M. M.; Lim, C. Y.; Koss, A. R.; Sekimoto, K.; Yuan, B.; Gilman, J. B.; Hagan, D. H.; Selimovic, V.; Zarzana, K. J.; Brown, S. S.; Roberts, J. M.; Müller, M.; Yokelson, R.; Wisthaler, A.; Krechmer, J. E.; Jimenez, J. L.; Cappa, C.; Kroll, J. H.; de Gouw, J.; Warneke, C. OH chemistry of non-methane organic gases (NMOGs) emitted from laboratory and ambient biomass burning smoke: evaluating the influence of furans and oxygenated aromatics on ozone and secondary NMOG formation. *Atmos. Chem. Phys.* **2019**, *19*, 14875−14899.
(43) Xu, L.; Crounse, J. D.; Vasquez, K. T.; Allen, H.; Wennberg, P. O.; Bourgeois, I.; Brown, S. S.; Campuzano-Jost, P.; Coggon, M. M.; Crawford, J. H.; Digangi, J. P.; Diskin, G. S.; Fried, A.; Gargulinski, E. M.; Gilman, J. B.; Gkatzelis, G. I.; Guo, H.; Hair, J. W.; Hall, S. R.; Halliday, H. A.; Hanisco, T. F.; Hannun, R. A.; Holmes, C. D.; Huey, L. G.; Jimenez, J. L.; Lamplugh, A.; Lee, Y. R.; Lindaas, J.; Neuman, J. A.; Nowak, J. B.; Peischl, J.; Peterson, D. A.; Piel, F.; Rickly, P. S.; Robinson, M. A.; Rollins, A. W.; Ryerson, T. B.; Sekimoto, K.; Selimovic, V.; Shingler, T.; Soja, A. J.; Clair, J. M.; Tanner, D. J.; Ullmann, K.; Veres, P. R.; Walega, J.; Warneke, C.; Washenfelder, R. A.; Weibring, P.; Wisthaler, A.; Wolfe, G. M.; Womack, C. C.; Yokelson, R. J. Ozone Chemistry in Western U.S. Wildfire Plumes. *Sci. Adv.* **2021**, *7*, No. eabl3648.
(44) Wang, S.; Coggon, M. M.; Gkatzelis, G. I.; Warneke, C.; Bourgeois, I.; Ryerson, T.; Peischl, J.; Veres, P. R.; Neuman, J. A.; Hair, J.; Singler, T.; Fenn, M.; Diskin, G.; Huey, L. G.; Ro Lee, Y.; Apel, E. C.; Hornbrook, R. S.; Hills, A. J.; Hall, S. R.; Ullmann, K.; Bela, M. M.; Trainer, M. K.; Kumar, R.; Orlando, J. J.; Flocke, F. M.; Emmons, L. K. Chemical tomography in a fresh wildland fire plume: A large eddy simulation (LES) study. *J. Geophys. Res. Atmos.* **2021**, *126*, No. e2021JD035203.
(45) Mota, B.; Wooster, M. J. A new top-down approach for directly estimating biomass burning emissions and fuel consumption rates and totals from geostationary satellite fire radiative power (FRP). *Remote Sens. Environ.* **2018**, *206*, 45−62.
(46) Wooster, M. J.; Roberts, G.; Perry, G. L. W.; Kaufman, Y. J. Retrieval of biomass combustion rates and totals from fire radiative power observations: FRP derivation and calibration relationships between biomass consumption and fire radiative energy release. *J. Geophys. Res.* **2005**, *110*, D24311.
(47) Wooster, M. J.; Zhukov, B.; Oertel, D. Fire radiative energy for quantitative study of biomass burning: derivation from the BIRD experimental satellite and comparison to MODIS fire products. *Remote Sens. Environ.* **2003**, *86*, 83−107.
(48) Freeborn, P. H.; Wooster, M. J.; Hao, W. M.; Ryan, C. A.; Nordgren, B. L.; Baker, S. P.; Ichoku, C. Relationships between energy release, fuel mass loss, and trace gas and aerosol emissions during laboratory biomass fires. *J. Geophys. Res. Atmos.* **2008**, *113*, D01301.
(49) Ellicott, E.; Vermote, E.; Giglio, L.; Roberts, G. Estimating biomass consumed from fire using MODIS FRE. *Geophys. Res. Lett.* **2009**, *36*, L13401.
(50) Roberts, J. M.; Stockwell, C. E.; Yokelson, R. J.; de Gouw, J.; Liu, Y.; Selimovic, V.; Koss, A. R.; Sekimoto, K.; Coggon, M. M.; Yuan, B.; Zarzana, K. J.; Browm, S. S.; Santin, C.; Doerr, S. H. The nitrogen budget of laboratory-simulated western US wildfires during the FIREX 2016 Fire Lab study. *Atmos. Chem. Phys.* **2020**, *20*, 8807−8826.
(51) Coggon, M. M.; Veres, P. R.; Yuan, K.; Koss, A.; Warneke, C.; Gilman, J. B.; Lerner, B. M.; Peischl, J.; Aikin, K. C.; Stockwell, C. E.; Hatch, L. E.; Ryerson, T. B.; Roberts, J. M.; Yokelson, R. J.; de Gouw, J. A. Emissions of nitrogen-containing organic compounds from the burning of herbaceous and arboraceous biomass: Fuel composition dependence and the variability of commonly used nitrile tracers. *Geophys. Res. Lett.* **2016**, *43*, 9903−9912.
(52) Nihill, K. J.; Coggon, M. M.; Lim, C. Y.; Koss, A. R.; Yuan, B.; Krechmer, J. E.; Sekimoto, K.; Jimenez, J. L.; de Gouw, J.; Cappa, C. D.; Heald, C. L.; Warneke, C.; Kroll, J. H. Evolution of organic carbon in the laboratory oxidation of biomass burning emissions. *Atmos. Chem. Phys.* **2023**, *23*, 7887−7899.
(53) Decker, Z. C. J.; Wang, S.; Bourgeois, I.; Jost, P. C.; Coggon, M. M.; DiGangi, J. P.; Diskin, G. S.; Flocke, F. M.; Franchin, A.; Fredrickson, C. D.; Gkatzelis, G. I.; Hall, S. R.; Halliday, H.; Hayden, K.; Holmes, C. D.; Huey, L. G.; Jimenez, J. L.; Ro Lee, Y.; Lindaas, J.; Middlebrook, A. M.; Montzka, D. D.; Neuman, J. A.; Nowak, J. B.; Pagonis, D.; Palm, B. B.; Peischl, J.; Piel, F.; Rickly, P. S.; Robinson, M.

https://doi.org/10.1021/acs.est.3c00537
Environ. Sci. Technol. 2023, 57, 13193−13204

A.; Rollins, A. W.; Ryerson, T. B.; Sekimoto, K.; Thornton, J. A.; Tyndall, G. S.; Ullmann, K.; Veres, P. R.; Warneke, C.; Washenfelder, R. A.; Weinheimer, A. J.; Wisthaler, A.; Womack, C.; Brown, S. S. Novel Analysis to Quantify Plume Crosswind Heterogeneity Applied to Biomass Burning Smoke. *Environ. Sci. Technol.* **2021**, *55*, 15646−15657.

(54) Majluf, F. Y.; Krechmer, J. E.; Daube, C.; Knighton, W. B.; Dyroff, C.; Lambe, A. T.; Fortner, E. C.; Yacovitch, T. I.; Roscioli, J. R.; Herndon, S. C.; Worsnop, D. R.; Canagaratna, M. R. Mobile Near-Field Measurements of Biomass Burning Volatile Organic Compounds: Emission Ratios and Factor Analysis. *Environ. Sci. Technol. Lett.* **2022**, *9*, 383−390.

https://doi.org/10.1021/acs.est.3c00537
Environ. Sci. Technol. 2023, 57, 13193−13204